McGrath, G., T. Kaeseberg, J. David Reyes Silva, J. W. Jawitz, F. Blumensaat, D. Borchardt, P.-E. Mellander, K. Paik, P. Krebs, P. S. C. Rao, (2019), Network topology and rainfall controls on the variability of combined sewer overflows and loads, Water Resources Research, doi:10.1029/2019WR025336.

Network topology and rainfall controls on the variability of combined sewer overflows and loads

Gavan McGrath[1,2,3,4], Thomas Kaeseberg[5], Julian David Reyes Silva[5], James W. Jawitz[6], Frank Blumensaat[7,8], Dietrich Borchardt[9], Per-Erik Mellander[1], Kyungrock Paik[10], Peter Krebs[5], P. Suresh C. Rao[11]

[1]Environment, Soils and Land Use Department, Teagasc, Johnstown Castle, Wexford, Ireland
[2]Ishka Solutions, Nedlands, 6009, Australia
[3]School of Agriculture and Environment, The University of Western Australia, Perth, 6000, Australia
[4]Department of Biodiversity Conservation and Attractions, Kensington, 6151, Australia
[5]School of Civil and Environmental Engineering, Technische Universität Dresden, Dresden, Germany
[6]Soil and Water Science Department, University of Florida, Gainesville, FL 32611, USA
[7]Eawag, Swiss Federal Institute of Aquatic Science and Technology, CH 8600 Dübendorf, Switzerland
[8]ETH Zurich, Institute of Environmental Engineering, 8093 Zurich, Switzerland
[9]Helmholtz Centre for Environmental Research UFZ, Magdeburg, Germany
[10]School of Civil, Environmental, and Architectural Engineering, Korea University, Seoul, South Korea
[11]Lyles School of Civil Engineering, Purdue University, West Lafayette, IN 47907, USA

Key Points:

- A parsimonious stochastic model is developed for CSO flows and solute fluxes.
- Uncalibrated stochastic model agrees with calibrated SWMM model.
- Network structure and rainfall control CSO load variability.

Corresponding author: Gavan McGrath, `gavan.mcgrath@uwa.edu.au`

This article has been accepted for publication and undergone full peer review but has not been through the copyediting, typesetting, pagination and proofreading process which may lead to differences between this version and the Version of Record. Please cite this article as doi: 10.1029/2019WR025336

Abstract

Water and pollutant fluxes from combined sewer overflows (CSO) have a significant impact on receiving waters. The random nature of rainfall forcing dominates the variability of sewer discharges, pollutant loads, and concentrations. An analytical model developed here, shows how sewer network topology and rainfall properties variously impact the stochasticity of CSO functioning. Probability distributions of sewer discharge and concentration compare well with the results from a calibrated Storm Water Management Model in an application to a sewershed located in Dresden, Germany. The model is determined by only four parameters, three of which can be predicted a priori, two from the rainfall record and one from the network topology using geomorphological flow recession theory, while the fourth can be estimated from a short discharge time series. The sensitivity of CSO and wastewater treatment loads to network structure suggests simple topologies may be more vulnerable to poor performance. The analytical model is useful for evaluating various CSO management strategies to reduce adverse impacts on receiving waters in a probabilistic setting.

1 Introduction

With a preference for human settlement next to rivers globally (Fang et al., 2018), wastewater discharges from urban areas have significant impacts on the health of riverine ecosystems and other human settlements downstream. A large number of cities globally have combined stormwater-sanitary sewer systems which discharge only mechanically treated sewage to aquatic and marine ecosystems during heavy rainfall. While urban wastewater treatment plants (UWWTPs) can take the majority of sewerage when present, combined-sewer overflow (CSO) discharges, rich in nitrogen, phosphorous, heavy metals, antibiotics, hormones and other sanitary pollutants, can have significant environmental impacts (David, Borchardt, von Tmpling, & Krebs, 2013; Phillips et al., 2012). Impacts on ecosystems arise from chemical (i.e. oxygen depletion, non-ionized ammonia peaks), and physical (i.e. frequently increased bed shear) stresses which depend to a large degree on local conditions (Borchardt & Sperling, 1997). Predicting the variability of CSO loads, concentrations and the frequency of events are key to understanding their impacts and for working towards resilient and sustainable urban drainage systems.

The variability of CSO functioning is a crucial component of its design. Key design criteria include: dilution rates in relation to dry weather flow; storage capacity in relation to design storms; an acceptable number of overflows per year; a maximum tolerable pollution load; and a maximum CSO discharge, among others (Riechel et al., 2016). Accounting for the stochastic nature of rainfall is one of the key challenges in CSO treatment design (Geiger, 1998). On the other hand, the sewer network controls the travel time distribution and also influences the flows and therefore the distribution of loads (Lhomme, Bouvier, & Perrin, 2004). In the following, the hypothesis that both rainfall variability and the sewer network topology are significant controls on the statistical properties of CSO functions are elaborated.

1.1 Rainfall Controls

Rainfall variability is a dominant control of CSO event timing, event loads, and concentration variability (Coutu, Giudice, Rossi, & Barry, 2012; Geiger, 1998; Sandoval, Torres, Pawlowsky-Reusing, Riechel, & Caradot, 2013). Short intense rainfall can promote elevated loads in first flush events (Krebs, Holzer, Huisman, & Rauch, 1999). Long duration, low intensity events can lead to poorer efficiency at an UWWTP, reducing the relative contribution of CSOs to river pollution (Phillips et al., 2012). Rainfall event intensities correlate with CSO water quantity and pollutant loads, while event duration and rain depth predict CSO pollutant concentrations (Sandoval et al., 2013). Under the changing climatic conditions, the frequency of intense rainfall may increase, which brings concerns about an increasing frequency of CSO events (Semadeni-Davies, Hernebring, Svensson, & Gustafsson, 2008; Sterk, de Man, Schijven, de Nijs, & de Roda Husman, 2016). These aspects of CSO performance are suited to treatment as a stochastic process, specifically accounting for the statistical properties of the timing and magnitude of rainfall events on the hydrological response (Botter, Porporato, Rodriguez-Iturbe, & Rinaldo, 2009).

1.2 Network Topology and Discharge Variability

Taking a nonlinear relationship between storage and runoff, Q, the continuity equation can be stated as (Botter et al., 2009):

$$\frac{dQ}{dt} = -kQ^{\alpha} + \xi(t) \tag{1}$$

where k is related to the hydraulic residence time, $0 < \alpha$ is a flow recession exponent. The rainfall, ξ, is assumed to follow a marked Poisson process with exponentially distributed times between events and event depths. From Eq. (1) the probability density function (pdf) for long-term temporal variability of Q was previously derived and the shape of the pdf was shown to be strongly controlled by α (Botter et al., 2009).

The topological properties of river networks have also been shown to be related to α (Biswal & Marani, 2014). Through a decomposition of a river network into so-called independent links, a power-law relationship between the number of independent links $N(l)$ and the total lengths of those same links, $G(l)$, at a distance l was derived: i.e. $N(l) \propto G(l)^{\alpha}$ (Biswal & Marani, 2010). In rivers, at least, there appears to be an intrinsic relationship between the network structure, the hydrological response and the variability of discharge.

Sewers share many topological characteristics with rivers (Yang et al., 2017). Like rivers, sewers follow power laws in the area-distance relationship (Hack´s Law) and in the probability distribution of contributing area, with exponent values similar to those found in rivers (Yang et al., 2017). A topological model also predicts runoff characteristics from sewers, as in rivers (Lhomme et al., 2004). We therefore hypothesize that the topological properties of gravity-driven sewer networks will influence the pdf of discharges, as well as pollutant loads and concentrations.

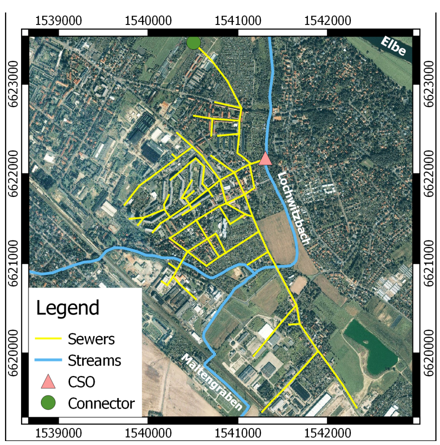

Figure 1. The Lockwitzbach sewer network and CSO. Coordinates are UTM Zone 33 North.

1.3 A Utilitarian Perspective

Clearly the structure of the sewer network and rainfall properties are important factors, together with regulations and/or guidelines, impacting upon CSO design and function. The manager of a sewer system might wonder what the use is to predict variability of a CSO system given that the rainfall properties cannot be controlled or that only small changes to the structure of a sewer system can be changed at any one time. Firstly, in response, many parts of the world face the challenge of constructing sewer systems to keep pace with rapid urbanization (Xu et al., 2019). As such there is a need for general design tools to plan future urban infrastructure as distinct from comprehensive hydrodynamic models solving the mass and energy balance equations for water and solute transport. Secondly managers of established systems more and more need to be aware of climate change impacts and to have a whole-of-catchment approach to managing sewer performance. This necessitates a systems-scale understanding of the transformation of rainfall variability into the variability of runoff production and sewer functioning.

Treating runoff as a stochastic process, has led to recent insights into how urbanization is changing the statistical properties of runoff as well as the variability of urban wash-off (Daly, Bach, & Deletic, 2014; Mejía, Daly, Rossel, Jovanovic, & Gironás, 2014). A stochastic approach was recently developed to evaluate the variability of water storage within, and discharges from a CSO tank (Wang & Guo, 2018). The process descriptions of storage and discharge used by Wang and Guo (2018) are identical to those used to previously examine soil water storage (McGrath, Hinz, & Sivapalan, 2007; Milly, 1993) and the temporal clustering of threshold flow events (Aquino, Aubeneau, McGrath, Bolster, & Rao, 2017; Laio, Porporato, Ridolfi, & Rodriguez-Iturbe, 2001; McGrath et al., 2007). Furthermore there have been recent advances in understanding how the network structure of rivers influences the hydrodynamics of discharge (Biswal & Marani, 2010). As a result, there is an opportunity to draw upon these new ideas in hydrology and apply them to improve the theoretical underpinnings of the practice of CSO management.

In this contribution we develop analytical expressions for the pdfs of CSO discharges, loads and concentrations with parameters derived from rainfall and the structure of the sewer network. The pdfs compare favourably with the results of a calibrated Storm Water Management Model (SWMM). The model developed here allows a sewer system manager/designer to easily assess how changing rainfall patterns (e.g. climate change scenarios) or urban growth (e.g., expansion and redesign of the sewer network) would impact CSO functioning and the risks to urban rivers.

2 Stochastic Analytical CSO Network Yield (saCSOny) Model

2.1 Discharges, Concentrations and Loads

The combined flows (and loads), Q_c (L_c) at a CSO diversion are given by the sum of the sanitary flow (load), Q_s (L_s), and urban stormwater flow (load), Q_u (L_u):

$$Q_c = Q_u + Q_s \tag{2}$$

$$L_c = C_c Q_c = L_u + L_s = C_u Q_u + C_s Q_s \tag{3}$$

where Q_u is the stochastic stormwater runoff, Q_s is the sanitary discharge, and C_u is the solute concentration in stormwater, assumed to be constant and much smaller than the steady concentration in the sanitary flow, C_s. Implicitly we assume $L_u \ll L_s$ and that the above terms represent system averages and thus describe well-mixed conditions at the catchment-scale. Sanitary flows typically display strong diurnal and weekly variability while stormwater flows vary significantly at sub-hourly time scales during rainfall events. While Q_s and C_s are initially assumed constant this assumption is later relaxed, such that fluctuations in the sanitary fluxes can be taken into account. The difference between Q_c and a threshold discharge, Q_t, at a CSO diversion, determines the CSO discharge, $Q_{CSO} = Q_c - Q_t$, and the load during a CSO event, $L_{CSO} = C_c Q_{CSO}$. The overflow structure is typically a weir and when the water level in the upstream pipe reaches a certain height, the weir overflows into the CSO pipes. These structures are constructed such that the flow directed towards the wastewater treatment plant depends on the upstream flow rate only to a minor extent. A simple threshold is therefore a good approximation to the hydrodynamics. The WWTP receives a flow, $Q_{WWTP} = Q_c - Q_{CSO}$, and a load, $L_{WWTP} = C_c Q_{WWTP}$. A stochastic model for Q_u is described next from which pdfs for the flows, loads and concentrations are derived.

2.2 Stormwater pdfs

Starting with Eq. (1), Botter et al. (2009) previously derived the pdf of discharges for rivers (the term Q_u here). In relation to Eq. (1), when $\alpha = 1$, the storage - discharge relationship is described as a linear reservoir, such that flows decrease exponentially with time during the recession phase. The pdf of Q_u in this case is given by Eq. (A.1). Flow recession in rivers, however, are often better described by power-laws (Wittenberg, 1999). When $0 < \alpha < 1$ the nonlinearity is termed concave; when $1 < \alpha < 2$, a range often observed in rivers, the nonlinearity is termed convex and finally, when $\alpha > 2$ the relation is termed hyperbolic. For concave recession the pdf is given by Eq. (A.2) (Botter et al., 2009). The pdfs of the convex and hyperbolic models have the same form as Eq. (A.2) without the Dirac delta term. For the variables of interest (Q_c, Q_{CSO}, Q_{WWTP}, C_c, L_{CSO}, and L_{WWTP}) we can apply a change of variables to derive their pdfs from the pdfs for Q_u (see Appendix A).

2.3 Accounting for Sanitary Discharge Variability

To take into account the diurnal variation in sanitary flows (Q_s) and concentrations (C_s), they can be treated as random variables,independent of Q_u and C_u. Using the marginal distribution rule, the pdf of Q_c is related to the marginal distribution of Q_c, given Q_s and the pdf of Q_s i.e.:

$$p_{q_c}\left(Q_c\right) = \int_0^\infty p_{q_c}\left(Q_c|Q_s\right) p_{q_s}\left(Q_s\right) \mathrm{d}Q_s \tag{4}$$

This is effectively a weighted average of the pdf of combined flows (Eq. A.4), where the weights are determined from the distribution of sanitary flows (p_{q_s}). A short period of observed dry-weather flows suffice to estimate p_{q_s}. The pdfs of discharges to the WWTP and from the CSO can be rescaled similarly. To derive the pdf of C_c the same approach can be used together with the distribution of sanitary loads, p_{L_s}, or alternatively the joint distribution of Q_s and C_s using the marginal distribution of C_c (Eq. A.10), and the joint pdf of Q_s and C_s i.e.:

$$p_{c_c}\left(C_c\right) = \int_0^\infty \int_0^\infty p_{c_c}\left(C_c|Q_s, C_s\right) p_{q_s c_s}\left(Q_s, C_s\right) \mathrm{d}Q_s \mathrm{d}C_s \tag{5}$$

Practically this is achieved by sampling a short time series of dry-weather flows $Q_s(t_i)$ and $C_s(t_i)$ at corresponding times then averaging the resulting ensemble of $p_{C_c}\left(C_c|Q_s(t_i), C_s(t_i)\right)$ over the set of samples, at each concentration, C_c, then normalizing the result to obtain a pdf. The complete set of equations are presented in Appendix A.

Next, the above model (defined by Eq 3-5 and A.1 - A.13, which we refer to as saCSOny) is applied to a sewershed located in Dresden, Germany. The software R was used for data analysis (R Core Team, 2018). All code used in this paper is documented in Supplementary Material) and the SWMM input and output needed to run the scripts can be found at `https://doi.org/10.26182/5bbbff6fadf94`. The R code includes scripts to numerically determine the pdfs and their corresponding cumulative distribution functions, analyse rainfall time series to determine the rainfall parameters, analyse SWMM input files to calculate α from the network properties, analyse a discharge time series to conduct flow recession analysis, and reproduce all figures in the main text and supplementary material.

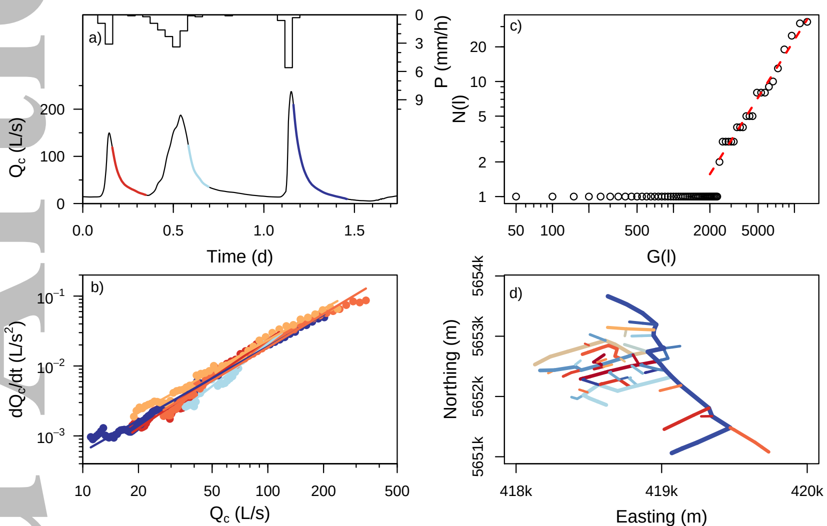

Figure 2. Empirical flow recession analysis: a) discharge, Q_c, and rainfall, P, time series for three of the five events shown in (b); b) Linear regression of the logarithms of the rate of change in discharge, and mean discharge, i.e. $log(-dQ_c/dt) = log(k) + \alpha log(Q_c)$ where the mean $\alpha = 1.7$ (Table S3); (c) The power law relation found between length and number of independent links i.e. $G(l) \propto N(l)^{1.7}$; and (d) The associated decomposed sewer network of independent links (color coded) (Biswal & Marani, 2014).

3 Application

3.1 The Lockwitzbach Sewershed

The Lockwitzbach sewer network, located in Dresden, Germany has a mean annual rainfall of 665 mm a^{-1} (1981-2010), a potential evaporation rate of 605 mm a^{-1} and a mean annual temperature of 9.4°C (Deutscher Wetterdienst, 2017). The sewershed has an area of 144.3 ha, with 36 ha of connected impervious surface. Wastewater from approximately 7,630 inhabitants and stormwater from primarily suburban land use is collected by 12.83 km of pipes. Extraneous water does not impact upon this sewer network Karpf and Krebs (2011). The CSO structure operates as a sideflow weir with a flow thresh-

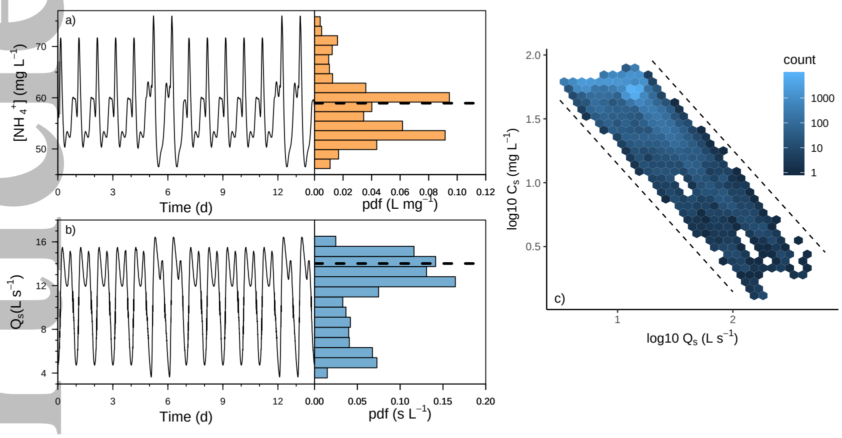

Figure 3. Characteristics of the sewer dynamics with: (a) Dry period discharges, Q_s (and pdf p_{q_s}); (b) concentrations, C_s ($[NH_4^+]$) (and pdf p_{c_s}); and (c) the $C_c - Q_c$ relationship, bounded by $C_c \propto Q_c^{-1}$.

old of approximately 600 L s^{-1}. Excess water is discharged into the Lockwitbach, an urban stream that drains into the Elbe River. A gate prevents backflow from the stream or downstream pipes. The northern outlet of the sewershed provides a connection for transport to the central Dresden WWTP.

A monitoring program of the joint Urban Observatory Dresden of Dresden University and the Helmholtz Centre for Environmental Research-UFZ under the Terrestrial Environmental Observation Initiative (TERENO) was established with the aims to analyze transport processes in sewer networks and the impacts of urban water management on river quality (Helm et al., 2015; Wollschlger et al., 2016). For hydraulic and water quality simulations the open source software EPA-SWMM v. 5.1.011 was previously calibrated to this data (Deb, Pratap, Agarwal, & Meyarivan, 2002; Kaeseberg et al., 2018; Rossmann, 2010; Steinberg, 2015). The calibrated model was run with a time step of ten minutes, using rainfall at a similar temporal resolution. A 17 year simulation was produced providing modeled discharge and ammonia concentrations at the CSO junction with a 10 minute resolution. Further details can be found in Supplementary Material (Text S2, Figures S1 and S2).

Table 1. saCSOny model parameters. [a]JFM rainfall parameters are listed with other seasonal parameters listed in Table S2. Mean values for dry-spell sanitary parameters are tabulated. The 95% confidence interval is denoted by ±.

Parameter	Value	Estimation method
λ	0.30 d^{-1}	Rainfall event analysis[a]
γ	0.54 mm^{-1}	
k	2 ± 0.03 mm$^{1-\alpha}$ d$^{\alpha-2}$	Flow recession.
α	1.7 ± 0.2	Flow recession & topology.
Q_s	11.3 L s^{-1}	Empirical pdf of dry spell flows.
C_s	57.2 mg L^{-1}	
C_u	0 mg L $^{-1}$	Assumed.

3.2 Parameter Estimation

The climate parameters, λ and γ, were determined from the precipitation time series (Supplementary Text S2, Table S2, Figures S3 - S5). These parameters describe the exponential probability distributions of the time between rainfall events and the magnitude rain events (Rodriguez-Iturbe, Porporato, Ridolfi, Isham, & Coxi, 1999). A minimum rainfall-free period of 5 h, selected as the threshold to delineate distinct rain events, was chosen based upon the flow recession characteristics which typically had returned to near pre-event flow rates within this time-frame. Due to the seasonality of rainfall the analysis was separated into annual quarters defined as January - March (JFM), April - June (AMJ), July - September (JAS) and October – December (OND). Precipitation totals for each event and the time between the start of events were determined and found to be approximately exponentially distributed for each quarter (Figures S3 and S4). The parameter λ was estimated by multiplying the frequency of actual rainfall by the long term runoff coefficient, 0.55. The parameters were estimated as the inverse of the mean of the time between rainfall events and the mean storm depth, respectively (Tables 2 and S2), equivalent to maximum-likelihood estimation. Potential for bias in the diurnal timing of events was assessed, with JFM and OND events distributed indistinctly from uniform distributions, indicating no bias in timing at a daily timescale (Figure S5). Events in AMJ and JAS were found to be significantly different from a uniform distribution by

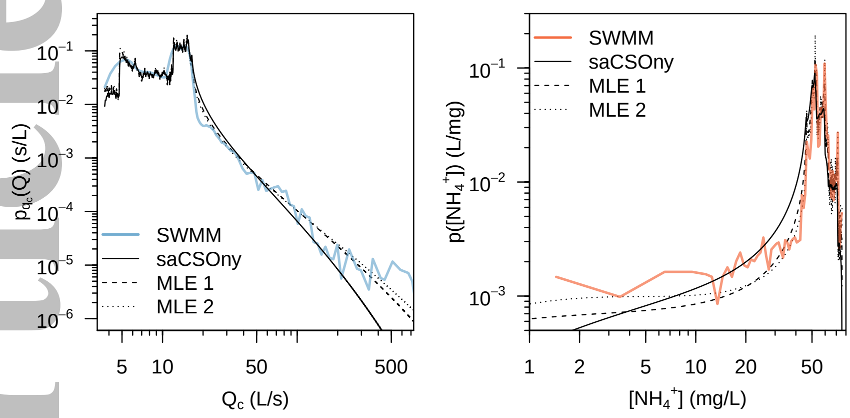

(a) (b)

Figure 4. Probability distributions of SWMM modeled and saCSOny predicted: (a) discharge, Q_c; and (b) concentration, C_c. Parameters as in Table 1. A posteriori fits of the pdf by maximum likelihood are also shown (MLE 1 where k was estimated with fixed $\alpha = 1.7$; and MLE 2 where both k and α were estimated, see Table S5).

the Kolmogorov-Smirnov (KS) test, with a preference for early to mid-morning events as compared to the late evening. While present, this bias had little impact on the estimated pdfs.

The point in the network chosen to represent combined flows was the junction immediately upstream of the pipe to the CSO structure (Figure 1). The parameters, k and α, were estimated from the mean of five flow recession events (Brutsaert & Nieber, 1977) (Figure 2, Table S3). Additional flow recession analyses were performed on 93 events (Table S4, Figure S6), selected with the criterion that the maximum discharge during the event was >160 L s^{-1} (i.e. approximately ten times the sanitary flow rate). Both analyses found a mean $\alpha = 1.7$ and mean $k = 2$ mm$^{1-\alpha}$ d$^{\alpha-2}$ (Table 1). A log-linear relationship (Figure S6c) between parameters was found between k and α. There was no evidence for a seasonal pattern in k or a normalized k (Dralle, Karst, & Thompson, 2015). The geomorphological approach of Biswal and Marani (2014) was applied to estimate α using the topology of the sewer network (Figure 2c,d). This independently resulted in the same value, $\alpha = 1.7$, as the mean measured recession exponent (Text S5). Separately, maximum likelihood estimation (MLE) was applied to estimate k (MLE 1) and both k and α (MLE 2) using p_{Q_c} (Table S5).

The sanitary discharge concentration has a characteristic diurnal and weekly periodicity (Figure 3a,b). A two-week long period of dry weather flows was used to determine Q_s and C_s, and from these their respective pdfs, p_{Q_c} and p_{C_c} (Text S6). Across the entire time series the C_c - Q_c relationship is bound by strong dilution (i.e. $C_c \propto Q_c^{-1}$) with the variation of dry weather concentrations preserved over several orders of magnitude of Q_c (Figure 3c), supporting the use of the well mixed assumption. Hysteresis is also evident, indicating that mixing is not perfect during individual events and thus apparently well mixed conditions emerge over the ensemble of flow events.

3.3 Predicted pdfs of CSO Function

The observed pdfs for JFM discharge and ammonia concentration [NH_4^+] agree well with the pdfs predicted from a priori estimated parameters (Figures 4; Figures S7 - S8, Text S7). A posteriori fits of the pdfs by MLE (Table S5) have very similar shapes. The multiple modes stem from the diurnal variation in sanitary flows and the roughness of the pdfs stem from the application of Eq. 5 using a fine discretization of the empirical pdfs of Q_s and C_s. Importantly, the pdfs capture the long tails of both distributions which is necessary to correctly capture the load distribution for CSO events.

Despite the similarity, one-sample KS tests reject the hypothesis that the empirical and model pdfs share the same distribution. As the KS tests develops statistics based upon the maximum deviation between the distributions, it is a conservative test. The failure of the test may stem from some clear differences between the two distributions. For discharge in the range of flows close to the upper end of sanitary flows (20 L s^{-1}) the saCSOny model tends to slightly over predict the likelihood of discharges. Similarly for concentrations near the lower end of sanitary concentrations (30 mg L^{-1}). The latter may be due to the over-prediction of discharges. Small to medium rainfall events of long-duration and low intensity, not well described as Poisson shocks, may be another contributing factor. Hydrodynamic processes such as storage, pipe friction, and hydrodynamic dispersion may also have an influence. Despite some minor deficiencies the simple model is able to capture significant features of the pdfs, from a just two weeks of observed dry-weather flows and a handful of flow recessions.

4 Sensitivity Analysis

In the following subsections the effects of the four model parameters are illustrated (Figures 4 - 6 and S9- S11). The values listed in Table 1 form the base scenario and sensitivity analysis is conducted by systematically varying the others.

4.1 Network and Hydrodynamic Controls

Flow recession has a significant impact upon CSO functioning (Figure 5). As α decreases the mode of p_{Q_c} increases near Q_s, intermediate flows become more probable and larger flows less likely (Figure 5a). The pdf p_{C_c} is a mirror image of p_{Q_c}, with lower concentrations less likely with higher α. For small α there is the potential for the pdf to become bimodal (Figure 5b). Interestingly the probability of high Q_{CSO} increases with decreasing α until $\alpha = 1$, and then with further decreases the probability of high discharges declines (Figure 5c). The frequency of CSO events first increases as α increases then for $\alpha > 1$ event frequency decreases again (Figure 5c). The distribution of WWTP discharges resembles that of Q_c, albeit truncated at the acceptance threshold, Q_t (Figure 5d). For the parameters used, the pdfs of CSO load are relatively uniform for $\alpha > 1$ indicating a wide range of loads are equally probable (Figure 5e). The load probabilities decrease and increase in accord the the frequency of CSO discharge. The likelihood of smaller loads to the WWTP changes similarly with , peaking at $\alpha \sim 1.5$ in this instance (Figure 5f).

Longer mean residence times (smaller k) increase the probability of larger combined flows, lower concentrations in combined flows, higher flows from CSOs, higher flows to WWTPs and higher loads (Figure 6). Of the hydrological parameters α is a key influence on the probability that a CSO is discharging (Figures 7). The parameter k, which controls hydrodynamic response times, influences the probability of CSO discharge at smaller values. The discharge threshold is also significant with declining likelihood of CSO discharge the higher the threshold and the higher the threshold the more significant are seasonal differences in the rainfall (Figure S9). Some variability of the discharge threshold could be expected to occur due to the hydraulics of pipe flow. Some variability is also due to discharge measurement errors, as practical CSO construction often differs from principles of weir design for the purposes of flow measurement (Ahm, Thorndahl, Nielsen, & Rasmussen, 2016). The effect of degree of variation in Q_t on the frequency of CSO discharge can be inferred from Figure S9. In the case of Lochwitzbach 10 20% variation in Q_t would produce small differences in the order of magnitude estimate of the CSO frequency. Smaller thresholds however would result in larger absolute errors.

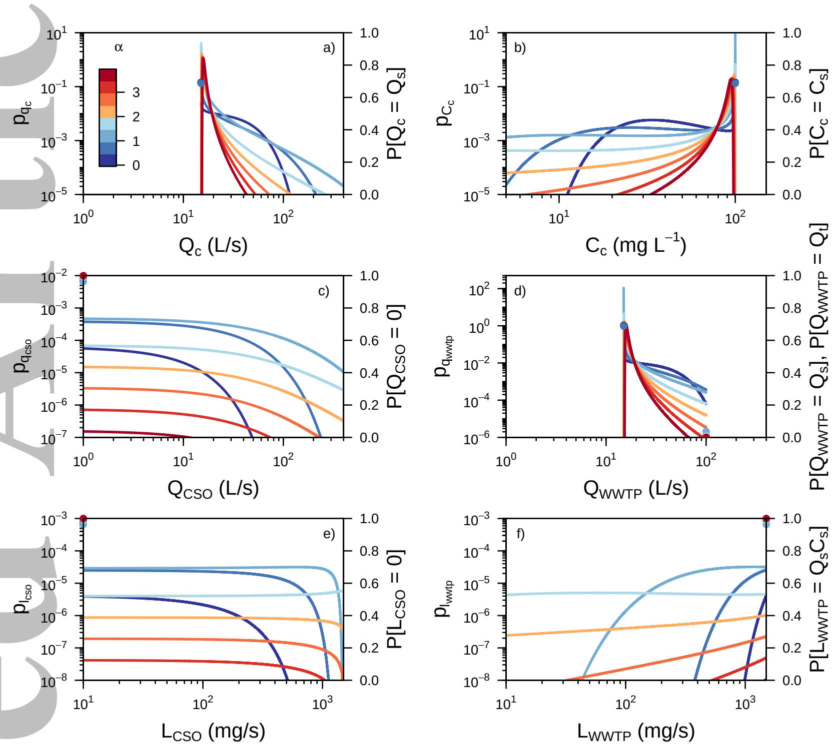

Figure 5. The impact of the flow recession parameter, α , on pdfs of: (a) Q_c; (b) C_c; (c) Q_{CSO}; (d) Q_{WWTP}; (e) L_{CSO}; and (f) L_{WWTP}. Parameters used: C_s = 100 mg L^{-1}, Qs = 15 L s^{-1}, Cu = 0 mg L^{-1}, k = 2 mm$^{1-\alpha}$ d$^{\alpha-2}$, γ = 0.45 mm^{-1}, λ = 0.3 d^{-1}; Q_t = 100 L s^{-1}. Lines denote the continuous part of the pdf (left axes) while the circles denote the atom of probability (right axes). For L_{cso} and Q_{cso} the points correspond to $L_{cso} = 0$ and $Q_{cso} = 0$.

4.2 Climate Controls

Rainfall has a significant impact on function, as expected. Increasing rainfall frequency (also increasing total annual rainfall) shifts the pdfs of C_c such that lower concentrations are more probable (Figure S10). This is in response to greater rainfall overall. The effect of increasing mean rain event depth ($1/\gamma$) is similar (Figure S11). Increasing rainfall frequency and mean rain event depth increases the probability of CSO events and higher loads as both contribute to greater overall rainfall (Figures 7b, S10, S11). The

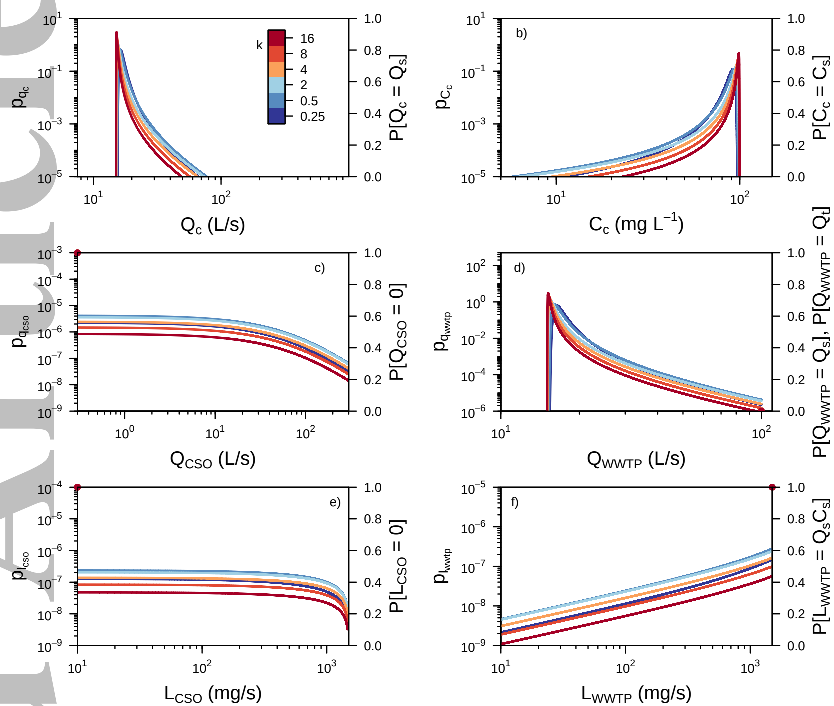

Figure 6. Sensitivity analysis to the flow recession parameter, k, with $\alpha = 1.7$. All other parameters as in Figure 5.

impact of fewer but more intense rainfall can be seen in the frequency of CSO events (Figure 7b). Climates of equal mean rainfall lie along lines with a slope of 1 in that figure, and it can be seen that a shift from a high frequency, low intensity rainfall to a low frequency higher intensity rainfall results in an increasing probability a CSO is discharging.

5 Discussion

The saCSOny model quantified relative roles of climate and network parameters in controlling the statistics of CSO functions. The important role of climate is well known. Perhaps less well recognized is the significant effect that the network topology has upon the variability of CSO functioning.

5.1 Network Controls

For Lockwitzbach at least it was demonstrated that the topology of the sewers could predict α. More work needs to be done to establish the extent to which this is more generally applicable to sewers. The empirical studies linking flow recession to topology have all been conducted on rivers to date (Biswal & Marani, 2014). With sewersheds evolving from simple linear features at early stages of development, towards fractal objects with topological properties of rivers, we expect α to change as they grow (Yang et al., 2017). Biswal and Marani (2014) suggested $\alpha \sim 1/(1-H)$, where $H \sim 0.6$ is Hack´s exponent. For sewers it has been shown H decreases from ~ 1 to 0.6 as they matured (Yang et al., 2017), which suggests α decreasing from ∞ to 2.5 during growth. While the relation suggested by Biswal and Marani (2010) may be valid for mature river networks, this suggests it may not be relevant for growing sewers. Intuition suggests that early on flow resembles a simple linear reservoir (i.e. $\alpha = 1$) and as the complexity of the network develops α likely increases. If this were the case the sensitivity analysis suggests that for the Lochwitzbach at least, high CSO loads and discharges tend to be more probable when $\alpha \sim 1$ (see Figure 4), thus poor performance of the CSO is more likely.

For k the expected changes seem to be clearer, as it is expected to decrease as the length of the pipe network and as the total area of connected impervious surface expands. The parameter k can be impacted by numerous factors. Longitudinal growth of the network would lengthen mean travel times of water and reduce k. Green infrastructure may also delay and lengthen travel times as a design goal. The results for Lockwitbach suggests that the frequency of CSO events would decline further were k to decrease.

A take-home message for a sewer manager is that alternative network structures will have varying flow recession exponents and, as a result, varying water quality outcomes. Designing the right structure, from a network perspective, has the potential to lower the costs and reduce the constraints to mitigate CSO impacts on receiving waters. The Lockwitzbach was the first sewer system in which α was predicted from the topology, so much more work needs to be done to evaluate this approach and identify its limitations in application to other sewersheds. Additionally, to design for growing infrastructure sewer manages would be further supported by providing them with knowledge as to how to design a network to achieve a set of hydrodynamic parameters as well as to predict how these properties age as the sewersheds self-organise over time (Semadeni-Davies et al., 2008).

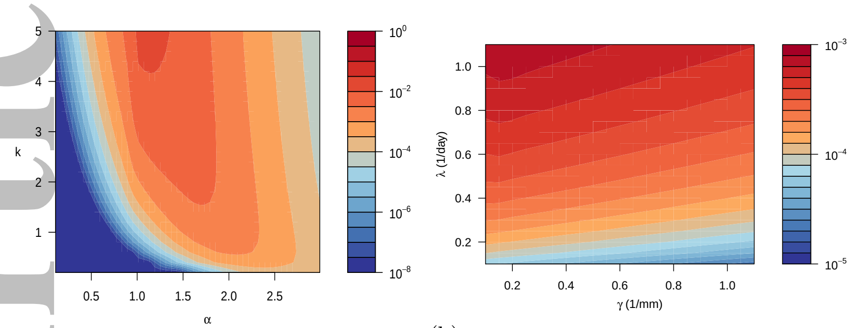

(a) (b)

Figure 7. Proportion of time (log10) a CSO discharges as a function of: (a) the topology/hydrodynamic parameters; and (b) the rainfall parameters. Parameters used include $Q_t = 100$ L s^{-1}, an impervious catchment area of 36 ha and for: (a) $\lambda = 0.3$ d^{-1}, $\gamma = 0.45$ mm^{-1}; and (b) $\alpha = 1.7$, $k = 2$ mm$^{-0.7}$ d$^{-0.3}$.

5.2 Climate Controls

Regional, seasonal and inter-annual variations in rainfall properties vary significantly and may explain large differences in CSO performance. We see (Figure 7) that increasing the likelihood of large rainfall events (smaller γ) leads to increased frequencies of CSO events Sterk et al. (2016). As the model assumes exponential distributions of rainfall depth and inter-even times it is best suited to describing what happens during typical conditions and may not be best at describing very rare events.

Catchment managers can't be expected to control the rainfall, as one reviewer pointed out, but it should be remembered that λ is an effective rainfall event rate, incorporating the filtering of smaller, non-productive events, and thus the runoff coefficient. Catchment managers can therefore directly influence the course of λ by supporting green infrastructure, pervious paving, and managing the connectivity of impervious area, amongst others actions. For example, green infrastructure can increase infiltration, increase detention storage, and reduce the peak flows of urban runoff, thereby reducing CSO loads (Riechel et al., 2016). Increased detention storage would decrease λ though not significantly impact γ (Rodriguez-Iturbe et al., 1999). A λ for green infrastructure, λ_g, can be estimated as: $\lambda_g = \lambda \exp(-\gamma s)$, where s is the effective catchment-scale detention storage added. In the case of Lockwitzbach the effect of adding an extra 1 mm of detention storage as green infrastructure would reduce the JFM λ from 0.3 d^{-1} to 0.17 d^{-1}. Assuming that α and k remain unchanged the frequency of CSO discharges would be expected to decrease approximately three-fold (Figures 7b, and S10). Natural multi-decadal variability as well as climate change related impacts on rainfall patterns have the potential to impact water quality outcomes (Mellander et al., 2018; Semadeni-Davies et al., 2008; Sterk et al., 2016). The saCSOny model offers the potential for sewer system managers to better plan for a mitigate these impacts.

5.3 Mixing Assumptions

The $C \propto Q^{-1}$ relationship, bounding the SWMM-simulated values (Figure 3), may be partly the result of the assumption in SWMM that individual pipes are completely mixed, high-dispersion reactors (Rossmann, 2010). This need not necessarily be the case at the scale of a sewershed, however in the case of the entire Lochwitzbach sewershed well-mixed conditions remain a reasonable approximation. Contrasting spatial distributions of stormwater and sanitary inflows likely determine to what extent complete mixing is a reasonable approximation (Krebs et al., 1999). Power law $C{-}Q$ relationships, $C = dQ^{-h}$ with $h < 1$, may be evidence of such incomplete mixing. Partial mixing could be introduced into Eq. 3 and distributions derived in a similar way (Text S1). Currently this would rely on an empirical $C - Q$ relationship to establish the mixing parameters which is somewhat unsatisfactory. As the flow recession exponent is estimated from the network topology it seems plausible that in the future related methods might be developed to predict d and h a priori, in a similar manner as has been done for flow recession (Biswal & Marani, 2014).

5.4 Assessing impacts on receiving waters

The pdf of CSO loads can be used to estimate impacts upon receiving waters. Where guidelines specify CSO loads with respect to dry flow rates in a river (Holzer & Krebs, 1998), then the pdfs of CSO load can be integrated to estimate the probability of not meeting a dilution threshold. Alternatively, where the river responds on much longer time scales, say several days to rise and fall from a single rainfall event, then the pdf of a dynamic load threshold can be estimated assuming load and river discharge are independent random variables in a manner similar to Eq. (4). In the case of the small Lockwitzbach stream, the discharges would be strongly correlated with the sewer flows at sub-daily time scales. In this case consideration of the covariance between stream and CSO discharges would be required. The size of the sewershed in relation to the receiving water should also be a consideration in assessing the applicability of the saCSOny model. It is expected small to medium, gravity-driven sewersheds, with a small number of outlets would be most suitable, however additional research comparing saCSOny predictions with sewer performance would help clarify the situations where the model is and is not suitable.

6 Conclusions

A four-parameter analytical model has been developed here to explore hydrological and climate factors influencing the functioning of a simple combined sewer overflow system. We demonstrated that three of the parameters of the model can be estimated readily a priori from the climate and the structure of the sewer network and one parameter from a short time series of observed discharge by flow recession analysis. A significant finding is that the flow recession exponent may be estimated from the sewer topology, and it significantly impacts variability of CSO function. This suggests that the statistical properties can be estimated from the design and a minimum of data without the need for solution of the full de Saint-Venant equations. Furthermore, relative contributions to variability from rainfall and the hydrodynamics/sewer structure can be disentangled. The equations derived here offer new approaches to rapidly assess options to mitigate CSO impacts on urban rivers. Future work is required to test the saCSOny model across diverse urban settings.

A The saCSOny Model

The pdf for stormwater discharge in the case of linear case is (Botter et al., 2009):

$$p_{q_u}(Q_u) = \frac{\gamma^{\frac{\lambda}{k}} Q_u^{\frac{\lambda}{k}-1}}{\Gamma\left(\frac{\lambda}{k}\right)} \exp\left[-\gamma Q_u\right] \tag{A.1}$$

and for the nonlinear case (Botter et al., 2009):

$$p_{q_u}(Q_u) = \frac{K}{Q_u^{\alpha}} exp\left[-\frac{\gamma}{k}\frac{Q_u^{2-\alpha}}{2-\alpha} + \frac{\lambda}{k}\frac{Q_u^{1-\alpha}}{1-\alpha}\right] + K\frac{k}{\lambda}\delta(Q_u) \tag{A.2}$$

Using Eq. A.2 the remaining pdfs for flows, loads and concentrations for the nonlinear case (the linear case is omitted for space as it can be derived similarly) can be derived using a change the variables, i.e.:

$$p_y(Y) = p_x\left(f^{-1}(Y)\right)\left|\frac{\partial f^{-1}}{\partial Y}\right| \tag{A.3}$$

where $f^{-1}(Y)$ is the inverse of a function $Y = f(X)$ of a random variable, X, with probability density, $p_x(X)$, and $p_y(Y)$ is the pdf of Y. Applying a change of variables in the case of the combined flows i.e. $Q_c = Q_s + Q_u$, gives the pdf of Q_c, as:

$$p_{q_c}(Q_c) = KG(Q_c - Q_s) + K\frac{k}{\lambda}\delta(Q_u) \tag{A.4}$$

where:

$$G(x) = \frac{1}{x^{\alpha}} exp\left[-\frac{\gamma}{k}\frac{x^{2-\alpha}}{2-\alpha} + \frac{\lambda}{k}\frac{x^{1-\alpha}}{1-\alpha}\right] \tag{A.5}$$

The remaining pdfs are derived similarly. With a CSO event triggered when $Q_c > Q_t$ then the pdf of its discharge, Q_{CSO}, can be determined to be:

$$p_{q_{CSO}}(Q_{CSO}) = KG(Q_{CSO} + Q_t - Q_s) + P[Q_C < Q_t]\,\delta(Q_{CSO}) \tag{A.6}$$

where:

$$P[Q_C < Q_t] = \int_0^{Q_t} p_{q_c}(Q_c)\,\mathrm{d}Q_c \tag{A.7}$$

The pdf for Q_{WWTP} is:

$$p_{q_{WWTP}}(Q_{WWTP}) = KG(Q_{WWTP} - Q_s) + P[Q_t < Q_c]\,\delta(Q_{WWTP} - Q_t) + P[Q_u = 0]\,\delta(Q_u) \tag{A.8}$$

where:

$$P[Q_t < Q_c] = \int_{Q_t}^{\infty} p_{q_c}(Q_c)\,\mathrm{d}Q_c \tag{A.9}$$

and $P[Q_u = 0]$ is given by the last term in Eq. (A.2). The pdf of the concentration of effluent is:

$$p_{C_c|Q_s,C_s}(C_c) = K\frac{|C_u - C_s|}{(C_u - C_c)^2}G\left(Q_s\left(\frac{C_s - C_c}{C_c - C_u}\right)\right) + P[Q_u = 0]\,\delta(C_s - C_c) \tag{A.10}$$

where we have written the pdf as a marginal distribution so as to recognize the possibility that Q_s and C_s may themselves display a degree of variability. While it is possible to derive the full pdf of CSO loads, for the sake of space and simplicity the case when the stormwater concentrations are negligible, i.e. $C_u \ll C_s$, is shown:

$$p_{l_{CSO}}(L_{CSO}) = K\frac{L_s}{(L_{CSO} - L_s)^2}G\left(\frac{L_s}{(L_s - L_{CSO})}Q_t - Q_s\right) + P[Q_u \leq Q_t]\,\delta(L_{CSO}) \tag{A.11}$$

where the sanitary load, $L_s = Q_s C_s$ has been substituted. The pdf of WWTP loads is:

$$p_{l_{WWTP}}\left(L_{WWTP}\right) = K\frac{Q_t L_s}{L_{WWTP}^2} G\left(\frac{L_s}{L_{WWTP}} Q_t - Q_s\right) + \tag{A.12}$$

$$P\left[Q_u \leq Q_t\right]\delta\left(L_s\right) \tag{A.13}$$

Acronyms

CSO Combined Sewer Overflow

UWWTP Urban Waste Water Treatment Plant

SWMM Stormwater Management Model

Acknowledgments

PSCR, PK, GM and DB received financial support from the National Research Foundation of Korea (NRF) (grant 2015R1A2A2A05001592) to attend the Synthesis Workshop Dynamics of Structure and Functions of Complex Networks, held at Korea University in 2015. PSCR was partially funded by the Lee A. Reith Endowment in the Lyles School of Civil Engineering at Purdue University. GM and PEM received additional support from the Diffuse Tools Project (grant 2016-W-MS-24) funded by the Environmental Protection Authority of Ireland. We thank Stadtentwaesserung Dresden for providing sewer network infrastructure and rainfall data and further acknowledge the work of several research assistants at TU Dresden who contributed to the development of the SWMM model and the collection of reference data. We would like to thank the two anonymous reviewers and the handling editor for their suggestions to improve the manuscript. Supporting data can be found at `https://doi.org/10.26182/5bbbff6fadf94`.

References

Ahm, M., Thorndahl, S., Nielsen, J. E., & Rasmussen, M. R. (2016). Estimation of combined sewer overflow discharge: a software sensor approach based on local water level measurements. *Water Science and Technology*, *74*(11), 2683-2696. doi: 10.2166/wst.2016.361

Aquino, T., Aubeneau, A., McGrath, G., Bolster, D., & Rao, S. (2017). Noise-driven return statistics: Scaling and truncation in stochastic storage processes. *Scientific Reports*, *7*(1). doi: 10.1038/s41598-017-00451-x

Biswal, B., & Marani, M. (2010). Geomorphological origin of recession curves. *Geophysical Research Letters*, *37*(24), n/a–n/a. doi: 10.1029/2010gl045415

Biswal, B., & Marani, M. (2014). 'universal' recession curves and their geomorphological interpretation. *Advances in Water Resources*, *65*, 34–42. doi: 10.1016/j.advwatres.2014.01.004

Borchardt, D., & Sperling, F. (1997). Urban stormwater discharges: ecological effects on receiving waters and consequences for technical measures. *Water Science and Technology*, *36*(8-9), 173–178.

Botter, G., Porporato, A., Rodriguez-Iturbe, I., & Rinaldo, A. (2009). Nonlinear storage-discharge relations and catchment streamflow regimes. *Water Resources Research*, *45*(10). doi: 10.1029/2008wr007658

Brutsaert, W., & Nieber, J. L. (1977). Regionalized drought flow hydrographs from a mature glaciated plateau. *Water Resources Research*, *13*(3), 637–643. doi: 10.1029/wr013i003p00637

Coutu, S., Giudice, D. D., Rossi, L., & Barry, D. (2012). Parsimonious hydrological modeling of urban sewer and river catchments. *Journal of Hydrology*, *464-465*, 477 - 484. doi: https://doi.org/10.1016/j.jhydrol.2012.07.039

Daly, E., Bach, P. M., & Deletic, A. (2014). Stormwater pollutant runoff: A stochastic approach. *Advances in Water Resources*, *74*, 148–155. doi: 10.1016/j.advwatres.2014.09.003

David, T., Borchardt, D., von Tmpling, W., & Krebs, P. (2013). Combined sewer overflows, sediment accumulation and element patterns of river bed sediments: a quantitative study based on mixing models of composite fingerprints. *Environmental Earth Sciences*, *69*(2), 479–489. doi: 10.1007/s12665-013-2447-3

Deb, K., Pratap, A., Agarwal, S., & Meyarivan, T. (2002). A fast and elitist multiobjective genetic algorithm: Nsga-ii. *IEEE Transactions of Evolutionary Computation*, *6*, 182–197. doi: 10.1109/4235.996017

Deutscher Wetterdienst. (2017). Retrieved from `https://www.dwd.de/EN/weather/weather_climate_local/`

Dralle, D., Karst, N., & Thompson, S. E. (2015). a, b careful: The challenge of scale invariance for comparative analyses in power law models of the streamflow recession. *Geophysical Research Letters*, *42*(21), 9285-9293. doi: 10.1002/2015GL066007

Fang, Y., Ceola, S., Paik, K., McGrath, G., Rao, P. S. C., Montanari, A., & Jawitz, J. W. (2018). Globally universal fractal pattern of human settlements in river networks. *Earth's Future*, *6*(8), 1134–1145. doi: 10.1029/2017ef000746

Geiger, W. F. (1998). Combined sewer overflow treatment - knowledge or speculation. *Water Science and Technology*, *38*(10), 1–8. doi: 10.2166/wst.1998.0366

Helm, B., Wiek, S., Krause, T., Weber, S., Kseberg, T., Zhang, J., & Krebs, P. (2015). *Das urbane observatorium dresden - integriertes monitoring fr ein verbessertes system-verstndnis in der siedlungswasserwirtschaft dresdner wasserbauliche mitteilungen.*

Holzer, P., & Krebs, P. (1998). Modelling the total ammonia impact of CSO and WWTP effluent on the receiving water. *Water Science and Technology*, *38*(10), 31–39. doi: 10.2166/wst.1998.0372

Kaeseberg, T., Kaeseberg, M., Zhang, J., Jawitz, J. W., Krebs, P., & Rao, P. S. C. (2018). The nexus of inhabitants and impervious surfaces at city scale — wastewater and stormwater travel time distributions and an approach to calibrate diurnal variations. *Urban Water Journal*, *15*(6), 576–583. doi: 10.1080/1573062x.2018.1529189

Karpf, C., & Krebs, P. (2011). Quantification of groundwater infiltration and surface water inflows in urban sewer networks based on a multiple model approach. *Water Research*, *45*(10), 3129–3136. doi: 10.1016/j.watres.2011.03.022

Krebs, P., Holzer, P., Huisman, J. L., & Rauch, W. (1999). First flush of dissolved compounds. *Water Science and Technology*, *39*(9), 55–62. doi: 10.2166/wst.1999.0441

Laio, F., Porporato, A., Ridolfi, L., & Rodriguez-Iturbe, I. (2001). Mean first passage times of processes driven by white shot noise. *Phys. Rev. E*, *63*, 036105. doi: 10.1103/PhysRevE.63.036105

Lhomme, J., Bouvier, C., & Perrin, J. (2004). Applying a GIS-based geomorphological routing model in urban catchments. *Journal of Hydrology*, *299*(3-4), 203–216. doi: 10.1016/s0022-1694(04)00367-1

McGrath, G. S., Hinz, C., & Sivapalan, M. (2007). Temporal dynamics of hydrological threshold events. *Hydrology and Earth System Sciences*, *11*(2), 923–938. doi: 10.5194/hess-11-923-2007

Mejía, A., Daly, E., Rossel, F., Jovanovic, T., & Gironás, J. (2014). A stochastic model of streamflow for urbanized basins. *Water Resources Research*, *50*(3), 1984–2001. doi: 10.1002/2013wr014834

Mellander, P.-E., Jordan, P., Bechmann, M., Fovet, O., Shore, M. M., McDonald, N. T., & Gascuel-Odoux, C. (2018). Integrated climate-chemical indicators of diffuse pollution from land to water. *Scientific Reports*, *8*(1), 944.

Milly, P. C. D. (1993). An analytic solution of the stochastic storage problem applicable to soil water. *Water Resources Research*, *29*(11), 3755-3758. doi: 10.1029/93WR01934

Phillips, P. J., Chalmers, A. T., Gray, J. L., Kolpin, D. W., Foreman, W. T., & Wall, G. R. (2012). Combined sewer overflows: An environmental source of hormones and wastewater micropollutants. *Environmental Science & Technology*, *46*(10), 5336–5343. doi: 10.1021/es3001294

R Core Team. (2018). Retrieved from `https://www.R-project.org/`

Riechel, M., Matzinger, A., Pawlowsky-Reusing, E., Sonnenberg, H., Uldack, M., Heinzmann, B., ... Rouault, P. (2016). Impacts of combined sewer overflows on a large urban river – understanding the effect of different management strategies. *Water Research*, *105*, 264–273. doi: 10.1016/j.watres.2016.08.017

Rodriguez-Iturbe, I., Porporato, A., Ridolfi, L., Isham, V., & Coxi, D. R. (1999). Probabilistic modelling of water balance at a point: the role of climate, soil and vegetation. *Proceedings of the Royal Society A: Mathematical, Physical and Engineering Sciences*, *455*(1990), 3789–3805. doi: 10.1098/rspa.1999.0477

Rossmann, L. A. (2010). Storm water management model user's manual version 5.0, epa/600/r-05/040 [Computer software manual]. US EPA. National Risk Management Research Laboratory, Cincinnati, Ohio, USA. Retrieved from `https://www.epa.gov/water-research/storm-water-management-model-swmm`

Sandoval, S., Torres, A., Pawlowsky-Reusing, E., Riechel, M., & Caradot, N. (2013). The evaluation of rainfall influence on combined sewer overflows characteristics: the berlin case study. *Water Science and Technology*, *68*(12), 2683–2690. doi: 10.2166/wst.2013.524

Semadeni-Davies, A., Hernebring, C., Svensson, G., & Gustafsson, L.-G. (2008). The impacts of climate change and urbanisation on drainage in helsingborg, sweden: Combined sewer system. *Journal of Hydrology*, *350*(1-2), 100–113. doi: 10.1016/j.jhydrol.2007.05.028

Steinberg, P. (2015). *Rswmm: Autocalibration for epa stormwater management model (swmm) version 5 using multi- or single objective optimization in r.* Retrieved from https://github.com/PeterDSteinberg/RSWMM

Sterk, A., de Man, H., Schijven, J. F., de Nijs, T., & de Roda Husman, A. M. (2016). Climate change impact on infection risks during bathing downstream of sewage emissions from CSOs or WWTPs. *Water Research*, *105*, 11–21. doi: 10.1016/j.watres.2016.08.053

Wang, J., & Guo, Y. (2018). An analytical stochastic approach for evaluating the performance of combined sewer overflow tanks. *Water Resources Research*, *54*(5), 3357–3375. doi: 10.1029/2017wr022286

Wittenberg, H. (1999). Baseflow recession and recharge as nonlinear storage processes. *Hydrological Processes*, *13*(5), 715-726. doi: 10.1002/(SICI)1099-1085(19990415)13:5⟨715::AID-HYP775⟩3.0.CO;2-N

Wollschlger, U., Attinger, S., Borchardt, D., Brauns, M., Cuntz, M., Dietrich, P., … Zacharias, S. (2016). The bode hydrological observatory: a platform for integrated, interdisciplinary hydro-ecological research within the TERENO harz/central german lowland observatory. *Environmental Earth Sciences*, *76*(1). doi: 10.1007/s12665-016-6327-5

Xu, Z., Xu, J., Yin, H., Jin, W., Li, H., & He, Z. (2019). Urban river pollution control in developing countries. *Nature Sustainability*, *2*(3), 158.

Yang, S., Paik, K., McGrath, G. S., Urich, C., Krueger, E., Kumar, P., & Rao, P. S. C. (2017). Functional topology of evolving urban drainage networks. *Water Resources Research*, *53*(11), 8966–8979. doi: 10.1002/2017wr021555